Instantaneous Responses of on-grid PV Plants to Changes in Environmental and Weather Conditions

Sayed Farzad Hosseini*, Behnam Mostajeran Goortani **‡, Mehdi Niroomand ***

* Renewable Energy Engineering Department, Faculty of Advanced Sciences and Technologies, University of Isfahan, Iran

** Renewable Energy Engineering Department, Faculty of Advanced Sciences and Technologies, University of Isfahan, Iran

*** Electrical Engineering Department, Faculty of Engineering, University of Isfahan, Iran

(Farzad_hosseini1991@ast.ui.ac.ir, b.mostajeran@ast.ui.ac.ir, Mehdi_niroomand@eng.ui.ac.ir)

‡ Corresponding Author; Second Author, Postal address, Tel: +98 9103450496

Fax: +98 31 37932129, b.mostajeran@ast.ui.ac.ir

Received: 11.06.2016 Accepted:23.07.2016

Abstract- The operation of an on-grid, 20 KW, PV, pilot plant is analysed. The instantaneous environmental variables and weather conditions including solar irradiance, temperature, wind speed, and clouds are recorded and analysed, simultaneously along with plant responses including PV module temperature, generated power, current, and voltage. The power decreases with increasing ambient temperature. Increasing solar irradiance increases the temperature difference between modules and ambient. Instantaneous energy and exergy efficiencies during three different days, representing sunny, partly cloudy, and cloudy days, are further calculated. The energy efficiency varies between 5.76% and 15.53%, while that of exergy varies between 4.84% and 15.73%. For cloudy days, the exergy efficiency is higher than that of energy, while for a sunny day it is in reverse. Another important parameter affecting the generated power is partial shading on PV modules, particularly during early mornings and late afternoons. The shading changes from 3% to 9%, because of small azimuth and elevation angles. It was found that partial shading of 4.73% on PV modules may result a significant power decrease of 52.3%. A new algorithm based on Fuzzy Logic is proposed to overcome these power decreases under partial shading.

Keywords PV cell; instantaneous respond; exergy and energy efficiency; partial shading.

1. Introduction

Nowadays, with increasing different sources of energy based on fossil fuels, the environment is polluted more than ever. Therefore, there is a critical need to renewable sources of energy such as Photo Voltaic (PV) cells, wind turbines, concentrated and non-concentrated solar power. A number of technologies to harvest solar energy are in progress and solar cells received more attention due to rapidly developing technology and potential applications to cover the energy demands of the developing world [1].

PV cells are the equipment that generate directly electricity from solar radiation. However, the operation and the efficiency of PV cells depend on the environmental and weather conditions such as temperature, solar irradiance, shading (from neighbour objects or from could), wind speed, moisture, and dust [2, 3].

In the present paper, the operation of an on-grid, 20 KW, PV plant is analysed under simultaneous changes in the environmental and weather conditions. The transient effects of variations in the environmental parameters such as solar irradiance, ambient temperature, module temperature, and wind speed on the generated power, voltage and current during three days of sunny, partially cloudy, and cloudy days, are presented. The exergy and energy efficiencies are further calculated. Moreover, a validated model developed in PSIM software, is used to calculate the effect of partial shading on the generated power. The measured data from the plant, temperatures and solar irradiance, are used as model inputs. The model output power is then compared with the measured generated power to calculate the effect of partial shading. Finally a new fuzzy logic algorithm is proposed to overcome the power reductions in PV cells under partial shading.

This paper is organized in eight sections. After introduction, in section two a literature review is presented. Section three describes the PV plant under study. Section four is about effect outdoor conditions on the plant parameters. The measured data are collected and analyzed during three days, representing partly cloudy, sunny, and cloudy days. In section five exergy and energy analysis are presented. Section six is about the effects of partial shading on the instantaneous generated power and efficiency. The last sections are discussion and conclusion.

2. Literature Review

Many works are presented so far to study the effect of environmental conditions on the performance of PV cells. The effects of humidity, wind speed, and dust on the efficiency of PV cells were determined by Mekhilef et al.[2]. They found that with increasing humidity power and efficiency decreases. Moreover, with increasing wind speed the module temperature decreases and the dust on the cells is swept away; therefore, the efficiency increases.

The results are shown that cell temperature has a significant effect on the photovoltaic parameters (such as open circuit voltage, short circuit current, maximum power, fills factor, and efficiency) and it controls the quality and performance of the solar cell. High temperature and low solar irradiance decreases the PV efficiency, and depending on the type of the cell. In Ref [1], the relative changes for mono-crystalline silicon are obtained from -0.0022/°C to -0.0025/°C, 0.002/°C, -0.0013/°C and -0.002/°C for open circuit voltage, short circuit current, fill factor and maximum output power respectively. For polycrystalline silicone cells, open circuit voltage reduction factor is (-79 mV/ºC) while that for the power is -25 W/ºC. Moreover, with increasing temperature, photocurrent increases to (0.045 %/ºC) because of reduction in bound gap [3]. In mono-crystalline silicone, these factors for power and fill factor are, respectively, (-0.2 %/ ºC) and (-0.65 %/ ºC [4]. Schwingshackl et al. [5] studied eight models to find about the effect of wind speed on cell temperature. For mono-crystalline silicon cells, Skoplanki 2 model represents best the module temperature estimation with considering the wind speed factor.

Power reduction, as a result of partial shading, is one of the common problems when using PV modules. Shading on PV modules, resulting from clouds, trees, buildings, objects, snow, dust, and even from front PV modules reduces the received solar radiation. In a PV module, depending on its' nominal voltage and current, there is a specific connection of series and parallel PV cells. Cells under partial shading act as a resistance and consume the generated electrical energy from un-shaded cells of the module. This energy is changed into heat and increases the module temperature and can even damage the cells. This problem is known as hot spot [6]. Also partial shading can result multi peaks in the characteristic current-voltage of PV cells. Consequently, the maximum power point tracking becomes more difficult [7]. Silvestre et al. [8] studied two pilots of 3 KW and 0.9 KW for one year. They showed that the shades resulting from neighbour tele-communications, buildings, and mountains can result power reductions of 6%, 20%, and 85%, respectively.

Various methods are reported in the literature to prevent or to reduce partial shading effect. A method is to bypass the cells under partial shading, using bypass diodes [7]. Yun Seng Lim et al. [9] purposed Dynamic Load Control (DLC) technique to increase power levels the PV system in shading condition in the cloudy region in Malaysia. Another technique to reduce the negative effects of partial shading is to use reconfigurable PV arrays/modules architecture [10, 11]. When an array/module is exposed to solar radiation, under partial shading conditions, different locations of the array/module receive different level of solar radiation. The total generated power from the array/module consequently will be limited to the modules/cells with the minimum power. To prevent this problem, Dynamic Photovoltaic Array (DPVA) technique is used. In this technique, modules/cells with similar shading conditions are connected together (reconfiguration), to prevent mismatch power losses between shaded and un-shaded modules/cells. Ref [12] presents a simple and efficient technique of module reconfiguration under partial shading.

DPVA technique is complex and expensive. A less expensive method is to select a suitable static PV array configuration that can improve the efficiency of PV systems by reducing mismatch losses. In Ref. [6] the performance of different photovoltaic array configurations, under various partial shading conditions, were studied: Series (S), Parallel (P), Series–Parallel (SP), Total-Cross-Tied (TCT), Bridge-Linked (BL), and Honey-Comb (HC). The obtained results proved the superiority of the TCT configuration which provides the best performances under most cases of partial shading conditions. A similar comparative study in [13] showed that TCT configurations results 3.8% increase in MPP compared to the SP configuration.

Energy and exergy analysis are two important tools to study the performance of PV cells. Energy analysis is based on the first law of thermodynamics, conservation of energy. Exergy analysis is based on the second law. Effects of irreversibilities such as working at high temperatures (higher than environment temperature) are included in the latter. Joshi et al. [14] studied the operation of two PV and PV/T plants in New Delhi. They showed that, depending on the solar radiation and weather conditions, exergy efficiency of PV plants changes between 7.8% and 13.85% while that of energy changes between 9% and 13%. Akyuz et al. [15] presented a new method to determine the exergy efficiency and observed that the exergy efficiency decreases with temperature and wind speed. For windy days, the exergy efficiency increases with an increase in solar radiation until it reaches the maximum point and then it decreases.

3. CASE STUDY: 20 KW SOLAR PV POWER PLANT

The PV pilot plant was established in May 2011 at the University of Isfahan, Iran (32º 61′ N, 51º 66′ E). The plant is composed of 108 mono-crystalline, 185 W PV modules (Suntech, China). The overall specifications of the plant and module specifications are listed in tables 1 and 2, respectively.

The generated power is connected to the grid via three one-phase inverters. Figure 1 shows a top view of the plant and the measurement equipment. The data including module temperature, ambient temperature, wind speed, and sun radiation intensity is continuously measured via a sensor box (SMA SUNNY SENSOR BOX) and sent to a webbox (SMA SUNNY WEBBOX). In the webbox data from the sensor box along with plant data (generated DC/AC power, DC/AC current, DC/AC voltage) are collected, recorded and sent to a computer.

The specifications of inverters and measuring devices including module temperature sensor, ambient temperature sensor, wind speed sensor, and solar radiation sensor are listed in table 3. The configuration of the modules is shown in Fig. 2. The modules are distributed in three arrays. Each array is composed of three parallel strings (N_s = 3). Each string is composed of twelve modules connected in series (N_m = 12).

According this configuration, the DC power (P_{DC}), DC current (I_{DC}), and DC voltage (V_{DC}) for each array and the total generated DC power can be calculated at STC:

$$P_{DC} = (12*36.4)*(3*5.09) = 6.7\ kW \quad (1)$$

$$V_{DC} = 12*36.4 = 436.8\ V \quad (2)$$

$$I_{DC} = 3*5.09 = 15.27\ A \quad (3)$$

$$P_{total} = 3*\ 6.7 \approx 20\ KW \quad (4)$$

In this paper, the instantaneous measured data are used, analysed, and reported during three different days, representing sunny day, partly cloudy day, and cloudy day of December 2, 10, and 20, 2014. The instantaneous exergy and energy efficiencies are further calculated and reported. Next, a validated model, developed in PSIM software, is used to calculate the generated power without partial shading. The measured data from the plant, temperatures and solar irradiance, are used as the PSIM model inputs, and the model output power is compared with the measured generated power under partial shading. At the end the monthly collective generated power in the year 2015 is reported.

Table 1. Overall specifications of the 20 KW pilot plant

Number of modules	Module angle	Number of modules in each string (N_m)	Number of strings in each array (N_s)	Number of arrays	Array power	Total power
108	3º to side South	12	3	3	6.67 kW	20 kW

Table 2. Technical specifications of PV modules

Parameters value	Con.efficiency	cells	I_{coeff}	V_{coeff}	P_{max}	I_{op}	I_{sc}	V_{op}	V_{oc}
	Up to 14.5 %	72	0.037%/°C	-0.34 %/°C	185W	5.09A	5.43A	36.4V	45V
STC: irradiance 1000 W/m^2, module temperature 25 °C, AM=1.5. NOCT: Irradiance 800 W/m^2, ambient temperature 20 °C, wind speed 1 m/s.									

Fig. 1. 20 KW PV pilot plant installed at the University of Isfahan Iran.

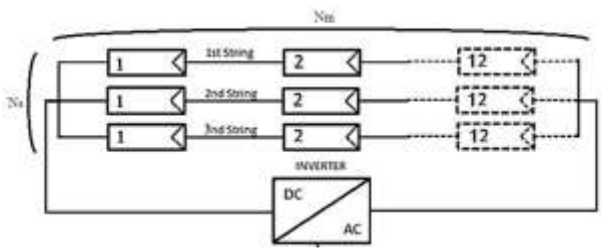

Fig. 2. Arrays configuration diagram

4. Effect of Outdoor Conditions on Plant Parameters

In this section, the effects of environment conditions during three days are presented. The effects of solar irradiance, ambient temperature, module temperature, and wind speed on the generated DC power, DC voltage and DC current are analysed and presented.

4.1. Effect of ambient and module temperatures

Fig. 3 shows the temperatures (ambient and module) and solar radiation variations during the three days. The ambient temperature, during the morning increases to its maximum at noon and then it decreases during the afternoon. At noon the maximum ambient temperatures for the days of December 2, 10, and 20 are 15.48 ºC, 16.28 ºC, and 28.13 ºC, respectively. Solar irradiance for the sunny day of December 10 increases from about 100 W/m^2 at 8 am to more than 800 W/m^2 at noon and again decreases to 100 W/m^2 at 4 pm.

Table 3. Specifications of the inverters and measurement equipment

Device	Model	Details
Inverter	SMA, Sunny Mini Central 7000TL	One phase , efficiency: 97.7-98% , max DC power: 7200W
Radiation sensor	SMA, Sensor box	Measurement range: 0 W/m^2 to 1500 W/m^2, accuracy: ± 8%
Module temperature sensor	SMA	Measurement range: -20°C to +110°C, accuracy: ± 0.5 %
Ambient temperature sensor	SMA	Measurement range: -30 to +80 °C, accuracy: ± 0.5 %
Wind speed sensor	SMA	Measurement range: 0.8 m/s to 40 m/s, accuracy: ± 0.5 %, Three axis , 2.5 meter above of land

Similar trend for the partly cloudy day of December 2 exists. However, because of presence of clouds between 10:30 am and 1:30 pm, the noon peak is not observed and there is a local minimum around 12 noon, where the maximum amount of clouds are in the sky. For the cloudy day of December 20, there is a reduction of sun radiation during the whole day. The radiation starts at 100 W/m^2 at 8 am, it increases to a maximum of 400 W/m^2 at 12 noon and again it decreases to 100 W/m^2 at 4 pm. There is a local minimum of 250 W/m^2 around 11:30 am, because of higher concentration of clouds at this time.

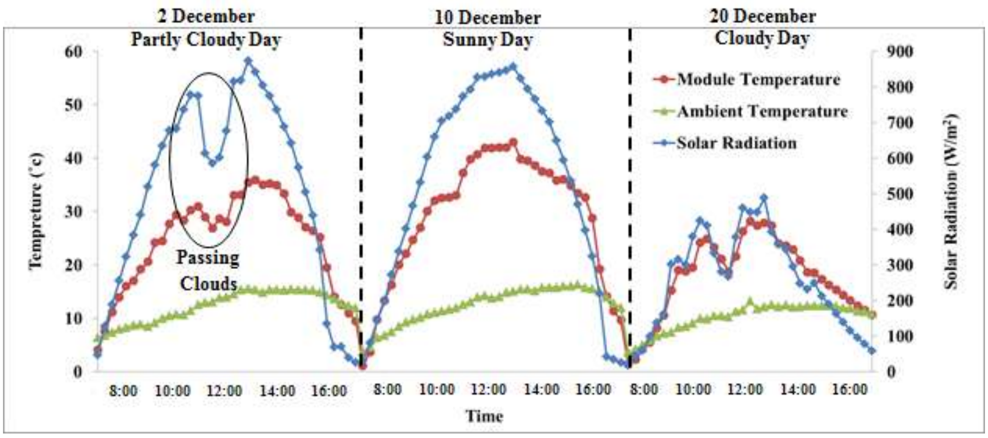

Fig. 3. Instantaneous solar irradiance, ambient temperature, and module temperature during partially cloudy, sunny, and cloudy days

According to Fig. 3, when solar irradiance increases, the difference between module temperature and weather temperature increases. Koehl et al. [16] found that there is a linear correlation between solar irradiance and the temperature difference, according to equation 5. They showed that the slope of the line depends on wind speed.

$$T_{mod} = T_{amb} + \frac{I_s}{I_{NOCT}}(T_{NOCT} - T_{amb}) \quad (5)$$

Where T_{mod} and T_{amb} are module temperature and ambient temperature, T_{NOCT} and I_{NOCT} are ambient temperature and solar irradiance at NOCT of 20 ºC and 800 W/m^2.

4.2. Effect of wind speed

According to Koehl et al. [17] at wind speeds in the order of 10 m/s, by increasing wind speed, the difference between ambient temperature and that of module temperature reduces. Consequently, the module energy efficiency increases as a result of reduction in module temperature. Fig. 5 shows wind speed variations during the three days. It is relatively low with a maximum of 2 m/s during the whole days. This low speed does not have considerable effect on module temperature (as shown in Fig.4).

4.3. Solar radiation and generated power

Fig. 6 compares the generated DC current, DC voltage, and solar irradiance during the three days. The same trend exists for current and solar irradiance during a day. For the sunny day, the current increases from less than 1 A at 8 am to a maximum of 14 A during the noon then it decrease to less than 1 A at 4 pm. For the partly cloudy day, because of higher concentration of clouds, there is a sudden decrease in the current around 11:30 am. The figure further indicates that the voltage remains at a constant of 420 V (with a maximum fluctuation of 10 V).

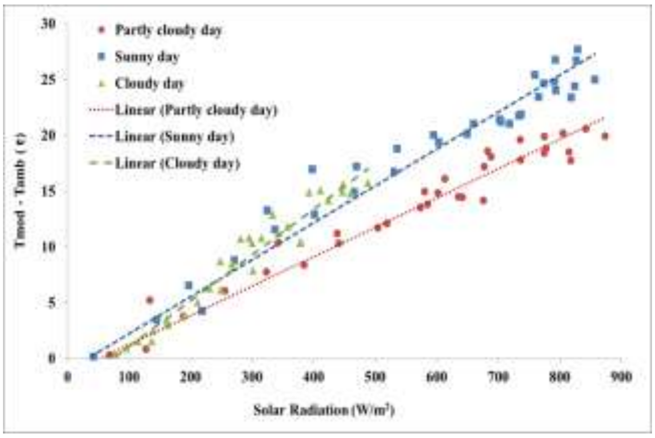

Fig. 4. Difference between ambient and module temperatures versus solar irradiance

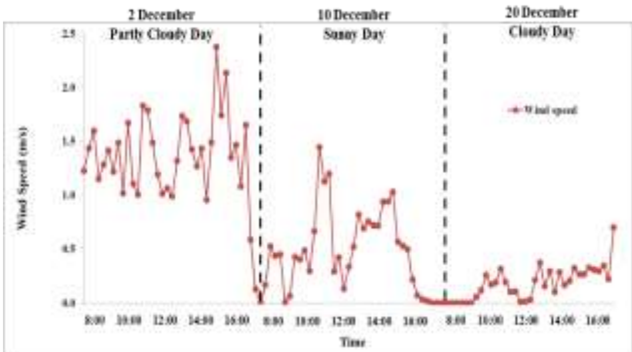

Fig. 5. Wind speed variations during the three days

5. Exergy and Energy Analysis of the PV Plant

Exergy analysis is a powerful tool to thermodynamically study energy systems. While, energy analysis is based on the first law of thermodynamics, exergy analysis is based on the second law. Effects of irreversibilities such as working at high temperatures (higher than environment) are included in the exergy analysis. These two analyses indicate the potentials of finding better systems, thermodynamically and economically [14]. Equation 6 is used to calculate the exergy of a given PV cell. The first term is electrical exergy and the second term is thermal exergy of a PV cell. Electrical exergy is the maximum electrical power of the system, and is equal to the voltage and current, corresponding to maximum power point (MPP). Thermal exergy includes the thermal losses from the cell surface and can be calculated from equation 8 [15]:

$$Ex_{PV} = Ex_{electrical} - Ex_{thermal} \tag{6}$$

$$Ex_{electrical} = V_m \times I_m \tag{7}$$

$$Ex_{thermal} = h_{ca}A(T_{cell} - T_{amb})(1 - \frac{T_{amb}}{T_{cell}}) \tag{8}$$

h_{ca} is convective heat transfer coefficient. The latter can be calculated from the wind speed v, according to equation 9:

$$h_{ca} = 5.7 + 3.8v \tag{9}$$

Combining equations 5 to 9 results:

$$Ex_{PV} = V_m \times I_m - h_{ca}A(T_{cell} - T_{amb})(1 - \frac{T_{amb}}{T_{cell}}) \tag{10}$$

Exergy efficiency of PV cell is:

$$Ex_{solar} = I_S A(1 - \frac{T_{amb}}{T_{sun}}) \tag{11}$$

Where I_s is total solar radiation (including direct and indirect intensities), T_{sun} is the sun temperature, usually equal to 6000 K. Therefore:

Where I_s is total solar radiation, T_{sun} is the sun temperature, usually equal to 6000 K. Therefore:

$$\eta_{Ex_{PV}} = \frac{Ex_{PV}}{Ex_{solar}} = \frac{V_m \times I_m - h_{ca}A(T_{cell} - T_{amb})(1 - \frac{T_{amb}}{T_{cell}})}{I_S A(1 - \frac{T_{amb}}{T_{sun}})} \tag{12}$$

Power conversion efficiency or energy efficiency of a PV cell, a measure of capability of the system to convert

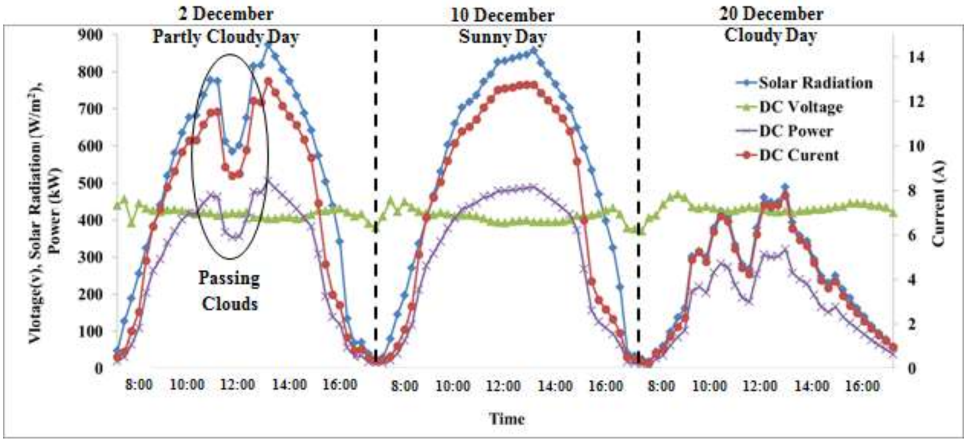

Fig. 6. Solar radiation, DC power, DC current, and DC voltage during representing partially cloudy, sunny, and cloudy days

solar energy to electrical, is defined according to equation 13.

$$\eta_{pc} = \frac{V_m \times I_m}{I_S A} \quad (13)$$

Fig. 7 shows the calculated exergy and energy efficiencies, according to equations 12 and 13, during the three days. The ranges of energy efficiency for partly cloudy, sunny, and cloudy conditions are, respectively, 5.9% -15.4%, 6.2%-15.4%, and 10.5%-15.8%. While those of exergy efficiency are, respectively, 6.0%-15.4%, 6.2%-15.3%, and 10.5%-15.9%.

It is important to note to the sharp fluctuations in the two efficiencies during a day. These fluctuations depend on instantaneous values of solar irradiance, module temperature, and shadow. The exergy efficiency for the cloudy day is 2% to 3% greater than that for sunny day. During the sunny day, solar irradiance is considerably higher than that of the cloudy day, and around noon, the sunny day irradiance reaches to two times of that in the cloudy day. However, because of lower temperatures of modules (10 ºC to 15 ºC) at the cloudy day, the exergy efficiency is higher. In other words, during cloudy days, PV modules perform better and convert higher proportion of the sun radiation into electrical power.

Another important point to note is the sudden decrease in the efficiencies (exergy and energy) from 14:15 to 15:00. This sudden decrease is a result of the partial shading of the front module arrays. As Fig. 7 indicates, from 14:15 to 15:00, there is a 50% decrease in the efficiencies which is a result of partial shading. To study this effect precisely and calculate its effect on power generation, next section is presented.

6. Effect of Partial Shading

6.1. PSIM model

PSIM software was used to simulate the plant. This software is used as a diagnosis tool to obtain the generated DC power, DC current and DC voltage when there is no shading on the modules. By comparing simulation results with the plant measured data under partial shading, the effect of partial shading on the generated power can be calculated. In this software, by setting technical specifications of the modules (according to table 4) and plant operating conditions (solar irradiance and module temperature) in the model, generated DC power, DC voltage, and DC current can be calculated. Fig. 8 shows the configuration of PV module arrays, DC/DC converter, MPPT charge controller as simulated in PSIM environment. According to this Fig., 36 modules are distributed in three strings of 12 modules. The simulation configuration is exactly the same as the real configuration of the PV modules in the plant.

Table 4. Technical specifications of the modules used in the PSIM model

Parameter	Value	Parameter	Value
Light Intensity at STC	1000 W/m^2	Number of Cells	72
Temperature at STC	25 ℃	Maximum Power (P_{max})	185 W
Band Energy (E_g)	1.12 eV	Voltage at P_{max}	36.4 V
Ideality Factor (A)	1.5	Current at P_{max}	5.09 A
Shunt Resistance (R_{sh})	500 Ω	Open Circuit Voltage (V_{oc})	45 V
Series Resistance (R_s)	0.0023 Ω	Short Circuit Current (I_{sc})	5.43 A
Saturation Current (I_{s0})	5.03e-7 A	Temperature Coff.of V_{oc}	-0.34 %/º C
Temperature Coefficient (C_t)	0.002 A/K	Temperature Coff.of I_{sc}	0.037 %/º C

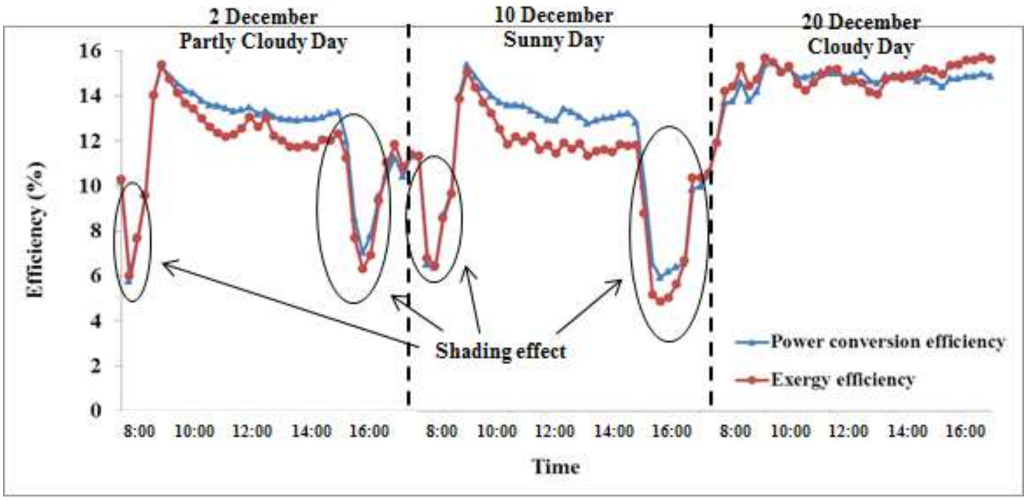

Fig. 7. Energy and exergy efficiencies during three days

Fig. 9 superposes the model calculated power and the measured power. As implied from the figure, except for the early mornings and the late afternoons, there are good agreements between the measured power and the PSIM model results with a maximum difference of 1%. Furthermore, the power difference between the graphs remains constant during a day. In PSIM simulations, the power drops because cable resistance and modules' internal resistances are not considered. Consequently, the calculated power in PSIM is slightly greater than that of plant measured data. The maximum power differences for sunny and cloudy days are 200 W and 50 W, respectively. The power differences depend on the amount of generated current. During sunny day the power loss is greater than that during cloudy day. This is because of higher electric currents and greater cable and modules' internal resistances during sunny day. Therefore, agreement between results of PSIM model and plant measured power is better during cloudy day.

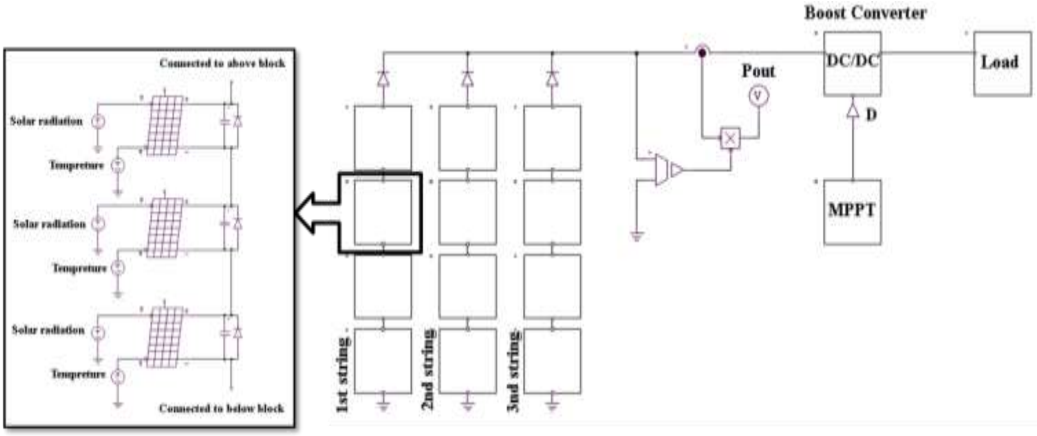

Fig. 8. Configuration of the modules used in PSIM model

During the early mornings and late afternoons of partly cloudy and sunny days, a significant difference exists between the results. There is partial shading of the neighbor buildings and trees on the modules; therefore, the output power decreases. Partial shading on the modules resulted about 100 W to 400 W reductions in the generated power, during the mornings. This reduction is even higher during the afternoons: 1.2 KW to 1.6 KW. These sudden reductions in the power do not exist for cloudy day because of the components of solar radiation and the absence of partial shading.

Solar radiation is composed of two components, diffuse radiation and direct radiation. For a brightest day, for example, with minimal amount of water steam, around 8% of the radiation is diffused. Near the polluted cities, this can reach to 22%. In addition to the diffused and direct radiations, the modules receive reflected diffused radiation. The latter is the reflected sun light from the environment surface. It depends on the reflection coefficient and horizontal angle. In a sunny day, direct radiation is the major part received on the modules, while for cloudy days, all received radiation is diffused radiation [17]. According to ElMghouchi [18], one of the best models to estimate the diffuse, direct, and total radiations is the Ghouard model:

$$I = I_0 . C_t . A_1 \, exp\left(-\frac{A_2}{\sin(h)}\right). \sin(h) \quad (14)$$

$$D = I_0 . C_t \left[0.271 - 0.2939. A_1 . exp\left(-\frac{A_2}{\sin(h)}\right)\right] \sin(h) \quad (15)$$

$$G = 0.271 I_0 . C_t . A_1 . \sin(h)$$
$$+ 0.706 I_0 . C_t . A_1 . \sin(h) \, exp\left(-\frac{A_2}{\sin(h)}\right) \quad (16)$$

$$C_t = 1 - 0.034\cos(j - 2) \quad (17)$$

$$h = sin^{-1}(\sin(\varphi) + \cos(\varphi) . \cos(\delta) . \cos(\omega)) \quad (18)$$

A_1, A_2 are determined from environmental and weather conditions. In sunny and partially cloudy days, the generated power is mostly resulted from direct radiation because A_1 is lower. On the other hand, during sunny days, shadows are

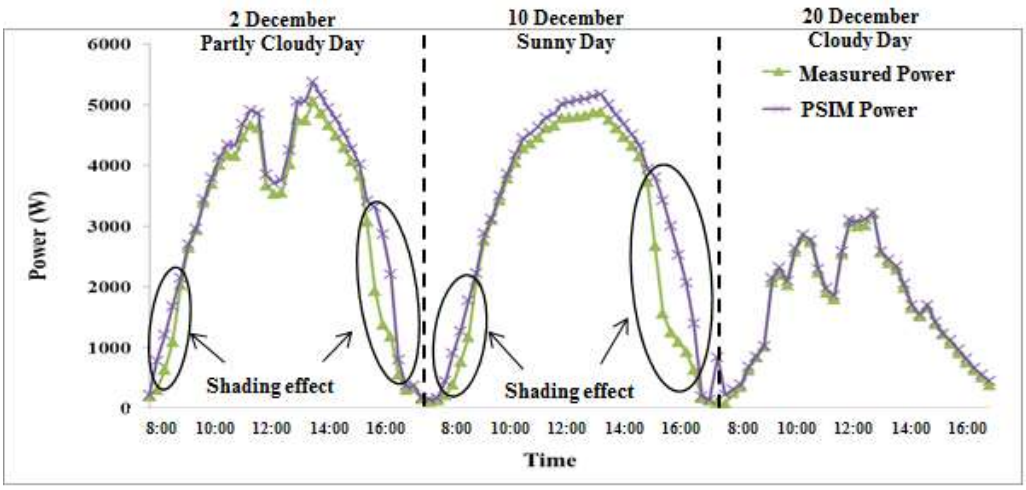

Fig. 9. PSIM simulation results and plant measure power during three days

formed therefore partial shading becomes important. During cloudy days, A_2 is greater than A_1 and there is no shading.

6.2 Partial shading during a sunny day

To calculate the effect of partial shading during mornings and afternoons, for a sunny day (21/11/2015), the percentage of the instantaneous shadow on the modules were measured by recording the images of modules and analyzing them. Fig. 10-a and 10-b show two images at 8:20 am and 15:25 pm, respectively. From morning to evening, the range of changes in the azimuth and elevation angles is 0–180º and 0–90º, respectively. Therefore, different shading patterns on the modules are formed during morning and afternoon. decreases to 4.3% and 119 W reduction in the generated power.

The maximum power drop is equal to 52.3% which is a result of a partial shading of 4.7% at 15:15. At this time 122.5 cells of a total of 2592 cells in array 2 are under shading. This type of partial shading results a significant power drop of 1415 W. Between 14:50 and 15:30, partial shading from the front modules has accrued. After 15:30 all cells are totally covered and partial shading disappears, because of shading of a neighbor mountain (Sofeh Mountain).

An important question arising here is how to design a

Fig. 10. Types and sources of shading on the module arrays a- morning shading b- afternoon shading

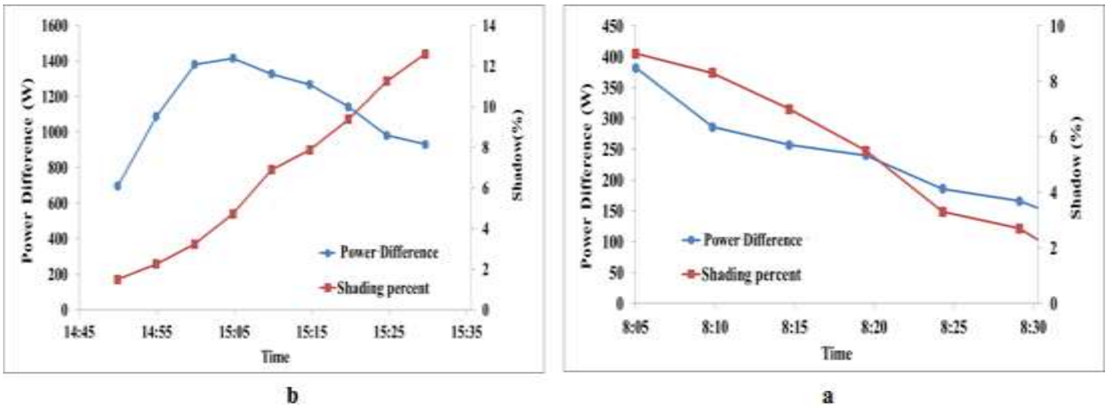

Fig. 11. Difference in power generation and partial shading for a sunny day a- morning b- afternoon

According to Fig. 10-a around 5.5% of the PV cells are covered by the shadow of neighbor trees at 8:20 am. At 15:25 pm 11.3% of the cells are covered by the shadow from front modules. Similar photos every 5 minutes were taken to obtain the data listed in Fig. 11-a and 11-b. The plant measured data were, simultaneously, recorded and the results are listed in table 5.

The power difference resulting from partially shading is calculated from equation 19:

$$Power\ Difference\ = P_{model} - P_{measured} \tag{19}$$

During the early morning, because of shadow from trees, the modules experience the negative effects of partial shading. At 8:05 am 9% of the cells are covered with the shadow, consequently, the generated power reduces from 2351W to 1969W, which is equal to 382.4 W, or 19.4% of reduction in the generated power. At 8:30 partial shading

controller for receiving maximum power from the modules under partial shading. The next chapter presents an algorithm for this purpose.

6.3 New algorithm of maximum power point tracking under partial shading

With respect to the characteristic P-V curve of the modules, maximum power point tracking (MPPT) controllers are proposed so far in the literature. An MPPT controller based on Fuzzy Logic has attracted more attention [19]. In this study, a new algorithm based on Fuzzy Logic is designed and used wherein it receives maximum power from the modules under partial shading.

By determining the effects of shading on the output power and P-V characteristic curve, the new MPPT method always guarantees maximum power point tracking of PV cells independent from environmental conditions, particularly, under partial shading conditions. The proposed approach has two stages. In the first stage, P-V curve of PV array is scanned by changing the duty cycle from minimum to maximum with fixed step. During the scanning, the maximum power and also corresponding voltage and duty cycle are saved and sent to the second stage. In the second stage, with the knowledge of the approximate location the global maximum point (GP) and sampling of power and voltage, Fuzzy logic controller is used to track the GP of PV array. In order to check the ability, speed and accuracy of the proposed MPPT method, the photovoltaic system is simulated with the proposed method. By changing conditions of the PV array and under worst-case conditions such as sudden changes in light intensity and different shadow patterns, the performance of the proposed method is evaluated. The simulation results confirm the good performance of the proposed approach in all conditions. Fig. 12 shows the diagram of the new algorithm.

kWh. A maximum energy of 3.53 MWh is generated in August and a minimum of 1.96 MWh generated in January. The maximum power generation is 16 KW. The total electricity generation is 105 MWh in 2015. The amount of CO_2 released into the atmosphere for difference types of power plants are listed in table 6 [20]. Compared to charcoal, oil, and natural gas power plants, this plant has prevented, respectively, the release of 88.4 ton, 72.7 ton, and 43.0 ton of CO_2.

Table 6. Amount of CO_2 released in power plants

Type of plant	CO_2 released (gCO_2/KWh)
Charcoal	800-1000
Oil	700-800
Natural gas	360-575
Mono crystalline PV	43-73

Table 5. Partial shading and generated power during morning and afternoon for 21/11/2015

Time	Solar radiation (W/m^2)	Real Power (W)	PSIM power (W)	Power difference (W)	Shaded area (%)	number of shaded cells	Power drop (%)
8:05	297.5	2351.4	1969	382.4	9	234	19.4
8:10	312.0	2358.3	2072	286.3	8.3	216	13.8
8:15	333.5	2476.7	2219	257.7	7	180	11.6
8:20	355.0	2476.1	2236	240.1	5.5	144	10.7
8:25	377.9	2709.0	2523	186.0	3.3	90	7.3
8:30	397.5	2482.8	2649	166.2	2.7	72	6.3
8:35	417.6	2908.8	2789	119.8	1	36	4.3
14:50	487.3	2501.9	3198	696.1	1.5	39	21.8
14:55	472.0	1994.0	3081	1087.5	2.3	58.5	35.3
15:00	444.9	1514.4	2895	1380.6	3.3	84	47.7
15:05	416.6	1289.9	2705	1415.1	4.7	122.5	52.3
15:10	389.3	1193.1	2521	1328.0	6.9	180	52.7
15:15	372.5	1138.4	2405	1266.6	7.9	204	52.7
15:20	344.7	1073.1	2216	1142.9	9.4	243	51.5
15:25	308.3	992.8	1975	982.2	11.3	291.5	49.7

It is important to know about performance and total generated power during a year. Fig. 13 shows the generated electrical energy in KWh from January to December 2015. The 20 KW pilot plant of the present study has generated, on the average, 2.75MWh energy each month. The daily average generation of the energy is between 60 kWh and 100

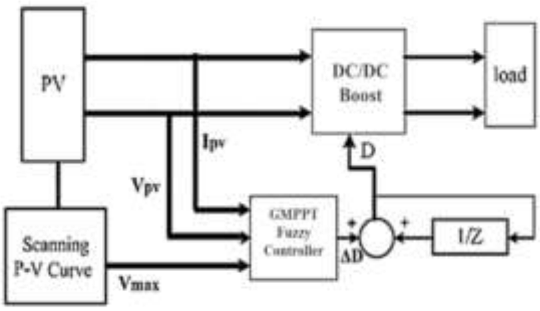

Fig. 12. Diagram of the new MPPT fuzzy logic

7. Discussion

From the above results it can be concluded that:

a. The total and the instantaneous generated power of a PV plant depend highly on the weather and environmental conditions.

b. In the analyzed PV plant the most important variable with time factors decreasing the power are respectively, partial shading, ambient temperature, and changes in solar irradiance.

c. During cloudy days modules temperature is lower; consequently, the efficiency of modules is higher.

d. The level of decrease in the power as a result of partial shading depends on the amount of the shadow and the pattern of the shadow. In other words, the number of by passed cells depends not only on the percentage of the shadow, but also on the shadow pattern on the modules. Consequently, in the studied PV plant, a 5% shadow from front modules results a 90% decrease in the generated power; while a 9% shadow from the threes resulted only 13.4% decrease in the power.

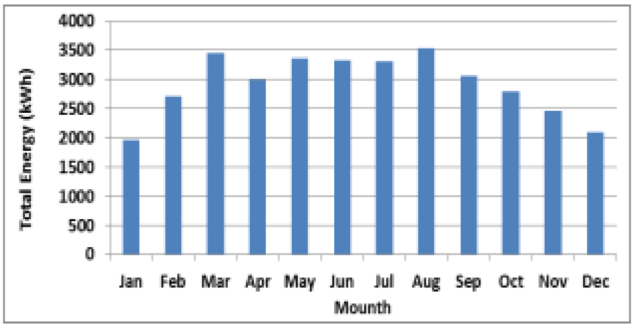

Fig.13. Monthly electrical energy production in 2015

8. Conclusion

The performance of an on grid 20 KW pilot PV power plant, under different environmental and weather conditions, is studied. The instantaneous effects of environmental parameters, namely, solar irradiance, ambient temperature, module temperature, wind speed, and partial shading are identified. It is shown that the instantaneous generated current is linearly proportional with solar irradiance. The generated power and the temperature difference between module and ambient increase with increasing solar irradiance. It was found that, the generated power does not depend on wind speed, because this parameter was very low. The instantaneous exergy and energy efficiencies are calculated during three days: sunny, partially cloudy, and cloudy days. The results indicated that, for cloudy day, the exergy of the system is 2%-3% higher than that of sunny day. This is because of higher amounts of differences between module and ambient temperatures during cloudy days. Partial shading during the early morning and afternoon, resulting from the environment trees and front modules, significantly reduces the generated power. A shading of about 5% resulting from front PV modules ends up with a power drop of more than 50 %. A new MPPT method is proposed that always guarantees maximum power point tracking of PV cells independent from environmental conditions, particularly, under partial shading. Cumulative data of the pilot plant in the year 2015 indicate that the plant has generated a total of 105 MWh and an average of 2.75MWh/month of electrical energy.

Acknowledgement

The authors acknowledge the financial support received from the Iran's Office of Vice-presidency for Science and Technology. Thanks to the efforts of Dr. M. Mostajaboddavati and Dr. M.R. Abdi. The financial support of the dean of research at the University of Isfahan is admired.

References

[1] S. Chander, A. Purohit, A. Sharma, Arvind, S.P. Nehra, and M.S. Dhaka, ''A study on photovoltaic parameters of mono-crystalline silicon solar cell with cell temperature'', Energy Reports, pp. 104-109, 2015.

[2] S. Mekhilef, R. Saidur, and M. Kamalisarvestani, ''Effect of dust, humidity and air velocity on efficiency of photovoltaic cells'', Renewable and Sustainable Energy Reviews , No. 5, pp. 2920-2925, 2012.

[3] F. Zaoui, A. Titaouine, M. Becherif, M. Emziane, and A. Aboubou, ''A Combined Experimental and Simulation Study on the Effects of Irradiance and Temperature on Photovoltaic Modules'', Energy Procedia, pp. 373-380, 2015.

[4] E. Radziemska, ''The effect of temperature on the power drop in crystalline silicon solar cells'', Renewable Energy, No. 1, pp. 1-12, 2003.

[5] C. Schwingshackl, M. Petitta, J.E. Wagner, G. Belluardo, D. Moser, M. Castelli, M. Zebisch, and A. Tetzlaff, ''Wind effect on PV module temperature: Analysis of different techniques for an accurate estimation'', Energy Procedia, pp. 77-86, 2013.

[6] F. Belhachat, and C. Larbes, ''Modeling, analysis and comparison of solar photovoltaic array configurations under partial shading conditions'', *Solar Energy*, pp. 399-418, 2015.

[7] J. Bai, Y. Cao, Y. Hao, Zh. Zhang, Sh. Liu, and F. Cao, ''Characteristic output of PV systems under partial shading or mismatch conditions'', Solar Energy, pp. 41-54, 2015.

[8] S. Silvestre, S. Kichou, A. Chouder, G. Nofuentes, and E. Karatepe, ''Analysis of current and voltage indicators in grid connected PV (photovoltaic) systems working in faulty and partial shading conditions'', *Energy*, pp. 42-50, 2015.

[9] Y.S. Lim, and J. H. Tang, ''Experimental study on flicker emissions by photovoltaic systems on highly cloudy region: A case study in Malaysia'', Renewable Energy, pp. 61-70, 2014.

[10] J.P. Storey, R.W. Peter, and D. Bagnall, ''Improved optimization strategy for irradiance equalization in dynamic photovoltaic arrays'', IEEE transactions on power electronics, No. 2946-2956, 2013.

[11] Y. Wang, X. Lin, Y. Kim, N. Chang, and M. Pedram, ''Architecture and control algorithms for combating partial shading in photovoltaic systems'', IEEE Transactions on Computer-Aided Design of Integrated Circuits and Systems, No. 6, pp. 917-930, 2014.

[12] S. Malathy, and R. Ramaprabha, ''Performance Enhancement of Partially Shaded Solar Photovoltaic Array Using Grouping Technique'', Journal of Solar Energy Engineering, No. 3, pp. 034505, 2015.

[13] D. Picault, B. Raison, S. Bacha, J. Aguilera, and J. De La Casa, ''Changing photovoltaic array interconnections to reduce mismatch losses: a case study'', In Environment and Electrical Engineering (EEEIC), 9th International Conference on, pp. 37-40. IEEE, 2010.

[14] Anand S. Joshi, I. Dincer, and Bale V. Reddy, ‘‘Thermodynamic assessment of photovoltaic systems’’, Solar Energy, No. 8, pp.1139-1149, 2009.

[15] E. Akyuz, C. Coskun, Z. Oktay, and I. Dincer, ‘‘A novel approach for estimation of photovoltaic exergy efficiency’’, Energy, No.1, pp.1059-1066, 2012.

[16] M. Koehl, M. Heck, S. Wiesmeier, and J. Wirth, ‘‘Modeling of the nominal operating cell temperature based on outdoor weathering’’, *Solar Energy Materials* and Solar Cells, No. 7, pp.1638-1646, 2011.

[17] J. Radosavljević, and A. Đorđević, ‘‘Defining of the intensity of solar radiation on horizontal and oblique surfaces on earth’’, Facta universitatis-series: Working and Living Enviromental Protection, No.1, p.77-86, 2001.

[18] Y.El Mghouchi, A.El Bouardi, Z. Choulli, and T. Ajzoul, ‘‘Models for obtaining the daily direct, diffuse and global solar radiations’’, Renewable and Sustainable Energy Reviews, pp. 87-99, 2016.

[19] Y. T. Chen, Y. C. Jhang, and R. H. Liang, ‘‘A fuzzy-logic based auto-scaling variable step-size MPPT method for PV systems’’, Solar Energy, pp. 53-63, 2016.

[20] D. Weisser, ‘‘A guide to life-cycle greenhouse gas (GHG) emissions from electric supply technologies’’, Energy, No. 9, pp.1543-1559, 2007.

NOMENCLATURE

P_{DC}	Generated DC power
V_{DC}	Generated DC voltage
I_{DC}	Generated DC current
P_{total}	Total generated power
V_{oc}	Open circuit voltage
I_{sc}	Short circuit current
P_{max}	Maximum Power
V_{coeff}	Temperature Coefficient of V_{oc}
I_{coeff}	Temperature Coefficient of I_{sc}
STC	standard test conditions
NOCT	Nominal Operating Cell Temperature
N_m	Number of modules in each string
N_s	Number of strings in each array
T_{amb}	Ambient Temperature
T_{mod}	Module Temperature
I_{NOCT}	Solar radiation at NOCT
T_{NOCT}	Ambient temperature at NOCT
Ex_{PV}	Exergy of PV
$Ex_{ectrical}$	Electrical exergy of PV
$Ex_{thermal}$	Thermal exergy PV
V_m	Maximum voltage
I_m	Maximum current
P_{DC}	Generated DC power
A	Surface area of solar cells
h_{ca}	Convective heat transfer coefficient
T_{cell}	Cell Temperature
T_{sun}	Sun temperature
E_g	Band gap energy
Ex_{solar}	Exergy of sun
η_{pc}	Power conversion efficiency of PV
I_0	Solar constant
R_s	Series resistance
I_s	Total Solar radiation
R_{sh}	Shunt resistance
ω	Hour angle
G	Global solar radiation flux on horizontal surface
I_d	Direct solar radiation flux on horizontal surface
D	Diffuse solar radiation flux on horizontal surface
C_t	Correction of the Earth–Sun distance
A_1	Turbidity factor depending on climatic conditions
A_2	Turbidity factor depending on climatic conditions
h	Solar elevation angle
φ	Latitude angle
η_{pc}	Power conversion efficiency of PV
I_0	Solar constant
R_s	Series resistance
I_s	Total Solar radiation
R_{sh}	Shunt resistance
ω	Hour angle
j	The day number of the year, ranging from 1 on 1 January to 365 on 31 December
G	Global solar radiation flux on horizontal surface
I_d	Direct solar radiation flux on horizontal surface
j	The day number of the year, ranging from 1 on 1 January to 365 on 31 December